Mon. Not. R. Astron. Soc. **000**, 1–9 (2011) Printed 16 December 2011 (MN LATEX style file v2.2)

Dead Zones around Young Stellar Objects: Dependence on Physical Parameters

Rebecca G. Martin[1], Stephen H. Lubow[1], Mario Livio[1] and J. E. Pringle[1,2]
[1] *Space Telescope Science Institute, 3700 San Martin Drive, Baltimore, MD 21218, USA*
[2] *Institute of Astronomy, Madingley Road, Cambridge, CB3 0HA, UK*

ABSTRACT
Angular momentum is transported outwards through an accretion disc by magneto-hydrodynamical (MHD) turbulence thus allowing material to accrete on to the central object. The magneto-rotational instability (MRI) requires a minimum ionisation fraction to drive turbulence in a disc. The inner parts of the disc around a young stellar object are sufficiently hot to be thermally ionised. Further out, cosmic rays ionise the surface layers and a dead zone forms at the mid-plane where the disc is too cool for the MRI to operate. The surface density in the turbulent active layer is often assumed to be constant with radius because the cosmic rays penetrate a constant layer. However, if a critical magnetic Reynolds number, $Re_{\rm M,crit}$, is used to determine the extent of the dead zone, the surface density in the layer generally increases with radius. For small critical magnetic Reynolds number of order 1, the constant layer approximation may be a reasonable fit. However, MHD simulations suggest the critical magnetic Reynolds number may be much larger, of order 10^4. Analytical fits for the surface density in the magnetic active layer show that $\Sigma_{\rm m} \propto Re_{\rm M,crit}^{-2} R^{9/2} T^2$, at temperature T and radius R, are a good fit for higher critical magnetic Reynolds number. For the metallicity variation between our galaxy, the LMC and the SMC, there should be no significant difference in the extent of the dead zone. Observations suggest an increase in the lifetime of the disc with decreasing metallicity that cannot be explained by the dead zone structure (ignoring possible differences in dust abundances).

Key words: accretion, accretion discs – planetary systems: protoplanetary discs – stars: pre-main-sequence

1 INTRODUCTION

Low-mass stars are thought to form from the free-fall collapse of a protostellar molecular cloud core to a protostar with a disc on a timescale of a few 10^5 yr (Shu, Adams & Lizano 1987). Angular momentum transport in accretion discs is driven by turbulence thus allowing material to accrete on to the young star. The magneto-rotational instability (MRI) can drive turbulence if the gas is well coupled to the magnetic field (Balbus & Hawley 1991). However, with a low ionisation fraction the MRI is suppressed (Gammie 1996; Gammie & Menou 1998). The inner parts of a disc around a young stellar object are hot enough to be thermally ionised. However, further out, the disc becomes layered with an MRI turbulent (active) layer at each surface and a dead zone at the midplane that is shielded from the ionizing radiation of cosmic rays and X-rays from the star (e.g. Sano et al. 2000; Matsumura & Pudritz 2003). In this work we concentrate on circumstellar discs, but note that dead zone formation is also favourable in circumplanetary discs (Martin & Lubow 2011a,b).

A frequently used assumption in calculations of discs with dead zones is that the surface density of the MRI active surface layer is constant with radius (e.g. Armitage, Livio & Pringle 2001; Zhu, Hartmann & Gammie 2009a; Terquem 2008; Matsumura, Pudritz & Thommes 2009). The cosmic rays enter the disc surface and are attenuated exponentially with a stopping depth of surface density around $100\,{\rm g\,cm^{-2}}$ (Umebayashi & Nakano 1981). However, this does not allow for recombination effects that may play a significant role in determining the ionisation of the disc.

A more realistic way to determine the dead zone is using a magnetic Reynolds number. MHD simulations show that magnetic turbulence cannot be sustained if the magnetic Reynolds number is lower than some critical value $Re_{\rm M} < Re_{\rm M,crit}$ (Fleming 2000). However, the critical value is uncertain. Simulations of Fleming (2000) that compute the non-linear outcome of instability suggest that $Re_{\rm M,crit} \approx 10^4$

without a net magnetic flux through the disc. With a magnetic flux it could be of the order of 100. Wardle (1999) and Balbus & Terquem (2001) considered the linear stability of the discs and find that the effects of Hall electromotive forces are important and the value may be as small as $Re_{\rm M,crit} = 1$. However, conditions for linear instability and for maintaining turbulence are not necessarily the same (Balbus & Hawley 2000). We consider a range of values for the critical magnetic Reynolds number from 1 to 10^4.

The surface layers of the disc may be ionised by cosmic rays or X-rays. Matsumura & Pudritz (2003) find that cosmic rays determine the extent of the dead zone under typical conditions unless the X-ray energy is very high. We consider only cosmic ray ionisation and neglect X-rays. Electrons in the disc are removed through dissociative recombination with molecular ions and at a slower rate with radiative recombination with heavy metal ions. The ionisation fraction, and hence the extent of the dead zone, is sensitive to the number of metal atoms because they quickly pick up the charges of molecular ions but slowly recombine with the electrons.

The typical life time of a protostellar disc in the solar neighbourhood, where the metallicity is $Z \approx 0.02$ is of the order of $3 - 5\,$Myr (e.g. Hernández et al. 2009). For stars near SN 1987A in the Large Magellanic Cloud (LMC) De Marchi, Panagia & Romaniello (2010) find from Hα fluxes that the mean lifetime is of the order of 13 Myr and the metallicity there is $Z \approx 0.008$. Note however, that these stars are likely to be slightly more massive. Similarly, De Marchi, Panagia & Romaniello (2011) observed the NGC 346 cluster in the Small Magellanic Cloud (SMC), where the metallicity is $Z \approx 0.002$, and find disc lifetimes of around 20 Myr. It appears from these results that the life time of the disc increases with decreasing metallicity. Dead zones affect the accretion rate through the disc and thus lifetime of disc accretion and so we consider how the dead zone varies with metallicity.

In Section 2 we describe the layered disc model where the extent of the dead zone is determined with the critical magnetic Reynolds number. We consider thermal ionisation, cosmic ray ionisation and recombination. In Section 3 we choose a fiducial disc model and find the dead zone and resulting accretion rate through the disc for varying metallicity and critical magnetic Reynolds number. We investigate the extent to which assuming a constant surface density in the active layer can approximate this and how sensitive the dead zone is to the metallicity. In Section 4 we find analytical approximations to the surface density in the active layer of the disc.

2 LAYERED DISC MODEL

In an accretion disc (Lynden-Bell & Pringle 1974; Pringle 1981) around a central object of mass M, where the material is in Keplerian orbits with angular velocity $\Omega = \sqrt{GM/R^3}$ at radius R, the kinematic turbulent viscosity may be parametrised by the α-prescription

$$\nu = \alpha \frac{c_{\rm s}^2}{\Omega} \tag{1}$$

(Shakura & Sunyaev 1973), where α is a dimensionless parameter that is not well constrained. Numerical simulations of MHD turbulence find $\alpha \gtrsim 0.01$ (Brandenburg et al. 1995; Stone et al. 1996; Fromang et al. 2007; Guan et al. 2009; Davis et al. 2009). Observational evidence from dwarf nova and X-ray outbursts suggests $\alpha \sim 0.1 - 0.4$ (King, Pringle & Livio 2007). In this work we take $\alpha = 0.1$ but discuss implications of a lower value. The sound speed is given by

$$c_{\rm s} = \sqrt{\frac{\mathcal{R}T}{\mu}}, \tag{2}$$

where T is the midplane temperature of the disc, $\mathcal{R}$ is the gas constant, $\mu = 2.3$ is the mean particle weight. The disc is viscous only in the turbulent active surface layer of the disc, not in the dead zone.

The dead zone is determined by where the MRI is unsustained because of poor coupling of the magnetic field to the disc. If turbulence is damped on a scale of λ, then the growth rate of the MRI is $V_{\rm A}/\lambda$, where $V_{\rm A} = B/(4\pi\rho)^{\frac{1}{2}}$ is the Alvén speed, B is the magnetic field and ρ is the density. Hawley, Gammie & Balbus (1995) use numerical simulations to find the shear stress due to turbulence induced by the instability to be $w_{r\phi} \approx \rho V_{\rm A}^2$. In terms of the Shakura & Sunyaev (1973) α-parameter this is $w_{r\phi} = \alpha\rho c_{\rm s}^2$ and so equating these we find $V_{\rm A} \approx \alpha^{\frac{1}{2}} c_{\rm s}$. The growth rate of the Ohmic diffusion is η/λ^2, where η is the diffusivity of the magnetic field. Complete damping occurs when all turbulence scales less than the scale height, $H = c_{\rm s}/\Omega$, are damped. This means that $\lambda < H$, or equivalently we can define the magnetic Reynolds number

$$Re_{\rm M} = \frac{\alpha^{\frac{1}{2}} c_{\rm s} H}{\eta}, \tag{3}$$

and the disc is dead if $Re_{\rm M}(R,z) < Re_{\rm M,crit}$. Note that several definitions of the magnetic Reynolds number have been used. For example, Fleming (2000) defined it as above but without the factor of $\alpha^{\frac{1}{2}}$. We consider a range of values for $Re_{\rm M,crit}$. The Ohmic resistivity is

$$\eta = \frac{234\,T^{\frac{1}{2}}}{x_{\rm e}}\ {\rm cm^2\ s^{-1}} \tag{4}$$

(Blaes & Balbus 1994), where the electron fraction is

$$x_{\rm e} = \frac{n_{\rm e}}{n_{\rm n}}, \tag{5}$$

where $n_{\rm e}$ is the number density of electrons and $n_{\rm n}$ is the total number density. With vertical hydrostatic equilibrium the number density is

$$n_{\rm n} = n_{\rm c} \exp\left[-\frac{1}{2}\left(\frac{z}{H}\right)^2\right], \tag{6}$$

where z is the height above the mid-plane of the disc. The number density at the midplane of the disc, where $z = 0$, is

$$n_{\rm c} = \frac{\Sigma}{\sqrt{2\pi}\mu m_{\rm H} H}, \tag{7}$$

where $m_{\rm H}$ is the mass of hydrogen. In the following two sections we consider the electron fraction in the disc with thermal ionisation, cosmic ray ionisation and recombination.

2.1 Thermal Ionisation

The dominant thermal ionisation ions in protostellar discs are Na^+ and K^+ (Umebayashi & Nakano 1981). However

the K^+ ion is more important at the onset of dynamically interesting ionisation levels because of its smaller ionisation potential. The Saha equation for the electron fraction from thermal ionisation can be approximated by

$$x_{\rm e} = 6.47 \times 10^{-13} \left(10^{[K/H]}\right)^{\frac{1}{2}} \left(\frac{T}{10^3\,{\rm K}}\right)^{\frac{3}{4}} \times \left(\frac{2.4\times10^{15}}{n_{\rm n}}\right)^{\frac{1}{2}} \frac{\exp(-25188/T)}{1.15\times10^{-11}} \quad (8)$$

(Balbus & Hawley 2000), where $[K/H] = \log_{10}(K/H) - \log_{10}(K/H)_{\rm solar}$ is the potassium abundance relative to hydrogen and $\log_{10}(K/H)_{\rm solar} = -7$. We consider the effect of varying $[K/H]$ in Sections 3.1. Thermal ionisation is most important in the inner parts of the disc where the temperatures are higher and it falls off exponentially.

2.2 Recombination

When thermal ionisation becomes negligible, the ionisation fraction is found with the balance of cosmic ray ionisation and recombination effects. Electrons may be captured by dissociative recombination with molecular ions (of density $n_{\rm M^+}$) and radiative recombination with heavy-metal ions (of density $n_{\rm m^+}$). Charge will be transferred from molecular ions to metal atoms and so the electron fraction depends also upon the metal fraction

$$x_{\rm m} = \frac{n_{\rm m}}{n_{\rm n}}, \quad (9)$$

where $n_{\rm m}$ is the number density of metals. The standard notation for metallicity is by mass fraction, Z. This is related to the metal fraction with

$$x_{\rm m} = \frac{Z}{\mu} \quad (10)$$

where μ is the average mass of a particle in units of the mass of hydrogen. For example, the molecule of highest mass taking part in the reactions may be CO, which has a mass of 28 units. In our galaxy $Z = 0.02$ so $x_{\rm m} \gtrsim 7\times10^{-4}$. In the LMC $Z = 0.008$ is equivalent to $x_{\rm m} \gtrsim 3\times10^{-4}$ and in the SMC $Z = 0.002$ is equivalent to $x_{\rm m} \gtrsim 7\times10^{-5}$.

Assuming the rates are the same for all species, the rate equation for the electron density is

$$\frac{dn_{\rm e}}{dt} = \zeta n_{\rm n} - (\beta_{\rm d} n_{\rm M^+} + \beta_{\rm r} n_{\rm m^+}) n_{\rm e} \quad (11)$$

and for the molecular ion density

$$\frac{d(n_{\rm M^+})}{dt} = \zeta n_{\rm n} - (\beta_{\rm d} n_{\rm e} + \beta_{\rm t} n_{\rm m}) n_{\rm M^+}. \quad (12)$$

The ionisation rate, ζ, is discussed in the next section. The recombination rate coefficients are

$$\beta_{\rm r} = 3\times10^{-11} T^{-\frac{1}{2}}\,{\rm cm^3\,s^{-1}} \quad (13)$$

for the radiative recombination of electrons with metal ions,

$$\beta_{\rm d} = 3\times10^{-6} T^{-\frac{1}{2}}\,{\rm cm^3\,s^{-1}} \quad (14)$$

for the dissociative recombination of electrons with molecular ions and

$$\beta_{\rm t} = 3\times10^{-9}\,{\rm cm^3\,s^{-1}} \quad (15)$$

for the charge transfer from molecular ions to metal atoms. Conservation of charge tells us that

$$n_{\rm e} = n_{\rm M^+} + n_{\rm m^+}. \quad (16)$$

Solving equations (11) and (12) in steady state with equation (16) gives the cubic equation

$$x_{\rm e}^3 + \frac{\beta_{\rm t}}{\beta_{\rm d}} x_{\rm m} x_{\rm e}^2 - \frac{\zeta}{\beta_{\rm d} n_{\rm n}} x_{\rm e} - \frac{\zeta\beta_{\rm t}}{\beta_{\rm d}\beta_{\rm r} n_{\rm n}} x_{\rm m} = 0 \quad (17)$$

(Oppenheimer & Dalgarno 1974; **?**; Millar Farquhar & Willacy) that can be solved to find the electron density. There are three solutions to equation (17) but only one that is both real and positive.

The solution to equation (17) can be simplified for the case where there is zero metallicity, $x_{\rm m} = 0$, and find

$$x_{\rm e} = \sqrt{\frac{\zeta}{\beta_{\rm d} n_{\rm n}}} \quad (18)$$

and also when the metals dominate so that $x_{\rm m} \gg x_{\rm e}$ and

$$x_{\rm e} = \sqrt{\frac{\zeta}{\beta_{\rm r} n_{\rm n}}} \quad (19)$$

(e.g. Matsumura & Pudritz 2003). We use these limits in Section 3. We note that this model does not take the effects of dust into account that may increase the size of the dead zone (e.g. Turner & Sano 2008; Okuzumi & Hirose 2011).

2.3 Cosmic Ray Ionisation

We consider the only external ionisation source to be cosmic rays with ionisation rate

$$\zeta = \zeta_0 \exp\left(-\frac{\Sigma_{\rm m}/2}{\chi_{\rm cr}}\right), \quad (20)$$

(where we have neglected the second term in the equation by Sano et al. 2000), $\zeta_0 = 10^{-17}\,{\rm s^{-1}}$ (Spitzer & Tomasko 1968) and $\chi_{\rm cr} = 100\,{\rm g\,cm^{-2}}$ (Umebayashi & Nakano 1981). The total surface density in the active layers is

$$\Sigma_{\rm m} = 2\mu m_{\rm H} \int_{z_{\rm crit}}^{\infty} n_{\rm n}\, dz = \Sigma\,{\rm erfc}\left(\frac{z_{\rm crit}}{\sqrt{2}H}\right), \quad (21)$$

where $z_{\rm crit}$ is the height of the disc above the mid-plane where the dead zone ends which we find in Section 2.5.

2.4 X-ray Ionisation

Young stellar objects may be active X-ray sources (e.g Koyama et al. 1994). However, Matsumura & Pudritz (2003) find that cosmic ray ionisation dominates X-ray ionisation. For example, comparing their figures 2 and 3 the dead zone is much larger in both height and radius with only X-rays. X-rays may dominate only if the energy is very high, $kT_{\rm X} = 5{-}10\,{\rm keV}$, but this is much higher than for most observed sources. In this work we neglect X-ray ionisation and concentrate on the effects of cosmic ray ionisation.

2.5 Dead Zone

We have found the electron fraction with thermal ionisation and cosmic ray ionisation with recombination. In order to determine the dead zone height we take the electron fraction

to be the maximum of equation (8) and the solution to equation (17). Now we can find the magnetic Reynolds number in equation (3) and for each radius, R, find the critical height in the disc, $z_{\rm crit}$ by solving $Re_{\rm M} = Re_{\rm M,crit}$. Where thermal ionisation is dominant, this is straightforward. However, it is slightly more complicated where cosmic ray ionisation dominates. For example, with the high metallicity limit for the electron fraction (equation 19) we solve

$$-\frac{1}{2}\left(\frac{z_{\rm crit}}{H}\right)^2 = \ln\left(\frac{\alpha^{\frac{1}{2}} c_{\rm s} H \zeta_0^{\frac{1}{2}}}{234\, T^{\frac{1}{2}} \beta_{\rm r}^{\frac{1}{2}} Re_{\rm M,crit} n_{\rm c}^{\frac{1}{2}}}\right)^2 - \frac{\Sigma/2}{\chi_{\rm cr}} {\rm erf}\left(\frac{z_{\rm crit}}{\sqrt{2}H}\right). \quad (22)$$

In the limit of low metallicity we replace $\beta_{\rm r}$ with $\beta_{\rm d}$. Given a total surface density and temperature, this equation can be solved numerically to find $z_{\rm crit}$ and hence the active layer surface density given in equation (21) and the dead zone surface density $\Sigma_{\rm d} = \Sigma - \Sigma_{\rm m}$. We illustrate this with an example in the next section.

3 DISC PROPERTIES

We choose a fiducial model for the disc structure around and star of mass $M = 1\,{\rm M}_\odot$ and consider properties of the dead zone. We take the total surface density to be

$$\Sigma = \Sigma_0 \left(\frac{R}{\rm AU}\right)^{-s}, \quad (23)$$

where $\Sigma_0 = 10^3\,{\rm g\,cm^{-2}}$ and the midplane temperature is

$$T = T_0 \left(\frac{R}{\rm AU}\right)^{-t}, \quad (24)$$

where $T_0 = 100\,{\rm K}$. We choose the disc such that without the dead zone, it has a constant accretion rate at all radii. This requires $\dot{M} \propto \nu\Sigma =$ const and so we take $s + t = 1.5$. Unless otherwise stated, we choose $s = t = 0.75$. This disc is in a steady state if it is supplied with a constant source of mass in the outer parts and the disc is fully MRI active. However, we now show that the disc may have a dead zone.

3.1 Active Layer

In Fig. 1 we show, at a fixed radius in the disc, $R = 1\,{\rm AU}$, the surface density in the active layer as a function of the total surface density. We vary the metallicity and critical magnetic Reynolds number in the disc. The dotted lines show the high metallicity limit for the electron fraction given in equation (19). The solid lines show intermediate metallicities found by solving the cubic equation (17) for the electron fraction. For fixed radius, the active layer reaches a constant surface density as the total surface density increases. The active layer is smallest with a low metallicity and a high critical magnetic Reynolds number.

However, the finite metallicities considered in Fig. 1 are tiny. Even the highest finite metal fraction we consider here, $x_{\rm m} = 10^{-7}$, corresponds to a very small metallicity of about $Z = 3 \times 10^{-6}$ (see equation 10) that is several orders of magnitude smaller than that in the SMC. The metallicity required for the dead zone to be significantly different from the high metallicity limit is very small, unless the critical magnetic Reynolds number is found to be significantly larger than 10^4. Hence, for reasonable metallicities, those in the observable universe, the dead zone structure does not depend on metallicity and the high metallitic limit is appropriate. In the rest of this work we consider only the high metallicity limit.

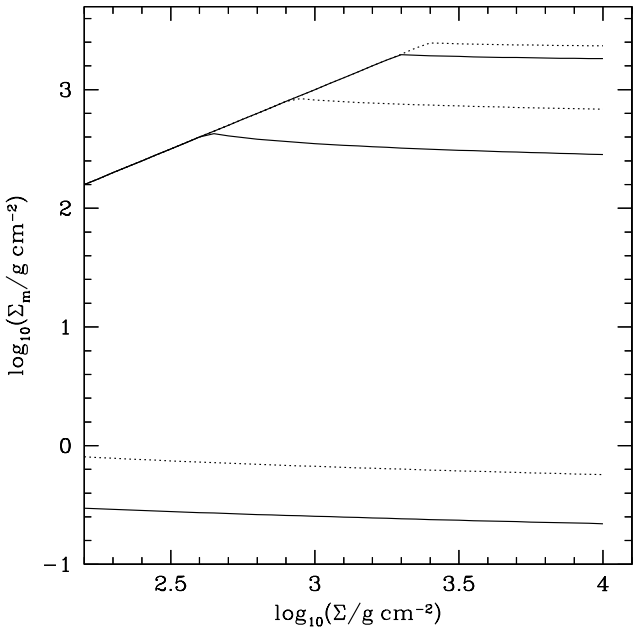

Figure 1. For a fixed radius in the disc of $R = 1\,{\rm AU}$, the surface density of the active layer in the disc is shown as a function of the total surface density. The upper two lines show $Re_{\rm M,crit} = 1$, the middle two lines show $Re_{\rm M,crit} = 100$ and the lower two $Re_{\rm M,crit} = 10^4$. The dotted lines show the high metallicity limit for the electron fraction found in equation (19) and the solid lines have $x_{\rm m} = 10^{-12}$ (upper solid line), $x_{\rm m} = 10^{-10}$ (middle solid line) and $x_{\rm m} = 10^{-7}$ (lower solid line) found by solving the cubic (17) for the electron fraction.

In Fig. 2 we show the height of the dead zone as a function of radius in the disc for varying critical magnetic Reynolds number in the high metallicity limit. As the critical magnetic Reynolds number increases, the size of the dead zone increases. The results are similar to those of Matsumura & Pudritz (2003) who find the dead zone in a disc with a different surface density and temperature distribution. In Fig. 3 we also plot the inner most parts of the dead zone and see that the effect of varying the constant $[K/H]$ (the Potassium abundance relative to hydrogen, see Section 2.1) is not very significant. It only affects the innermost parts of the disc where thermal ionisation is the dominant source. Further out where cosmic ray ionisation becomes dominant the dead zone does not depend on $[K/H]$. In the rest of the work we take the solar abundance value, $[K/H] = 0$.

In Fig. 4 we show the surface density of the active layer as a function of radius of the disc for varying critical magnetic Reynolds number in the high metallicity limit. The inner parts of the disc are thermally ionised and the outer parts are fully ionised by cosmic rays. Hence in these re-

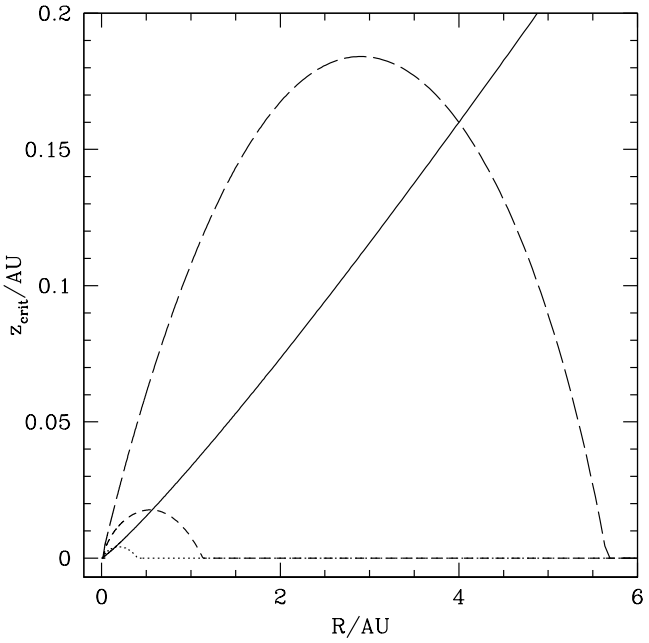

Figure 2. The height of the dead zone as a function of radius for critical magnetic Reynolds number of 1 (dotted line), 100 (short-dashed line) and 10^4 (long-dashed line) in the high metallicity limit. The solid line shows the scale height of the disc, H. Note that the axis scales are not the same.

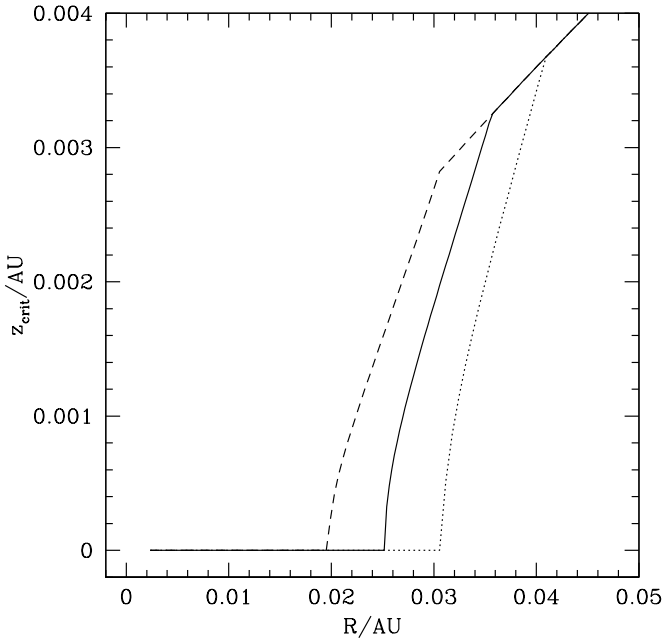

Figure 3. The height of the inner parts of the dead zone as a function of radius for a critical magnetic Reynolds number of 100 in each case with solar abundance, $[K/H] = 0$, (solid line, as used for the rest of the work), $[K/H] = 2$ (dotted line) and $[K/H] = -2$ (dashed line) in the high metallicity limit. The three dead zone heights are different where the electron fraction due to thermal ionisation (equation 8) is larger than that due to the cosmic ray ionisation (equation 19). At larger radii thermal ionisation becomes negligible and the dead zone is found with the cosmic ray ionisation that does not depend on the parameter a. Note that the scales of the axes are not the same.

gions, the surface density of the active layer is equal to the total surface density, $\Sigma_{\rm m} = \Sigma$.

In the region where a dead zone exists, the surface density in the active layer initially decreases sharply. This is because the temperature in the disc decreases with radius ($T \propto R^{-3/4}$) and the thermal ionisation decreases exponentially with temperature. However, once the ionisation through cosmic rays dominates the thermal ionisation, the active layer surface density increases with radius until the whole disc is turbulent. Independently, the decreasing temperature distribution has the effect of lowering the active layer surface density in this region. However, the dominant effect is the scale height of the disc, H, that increases with radius ($H \propto R^{9/8}$). As described in Section 2, the turbulence is completely damped when it is damped on all scales $< H$. The damping decreases with radius because of the increasing scale height and thus the active layer surface density increases.

The constant surface density in the active layer that is more generally assumed is also plotted in the dot-dashed line in Fig. 4. We take as an example a disc which is dead if $T < T_{\rm crit} = 1500\,{\rm K}$ and $\Sigma > \Sigma_{\rm crit} = 200\,{\rm g\,cm^{-2}}$. The active surface density determined by the critical magnetic Reynolds number is very different from a constant except for a the low critical magnetic Reynolds number. For $Re_{\rm M,crit} = 1$, the surface density of the active layer is close to constant but much larger than the generally assumed values that are less than around $200\,{\rm g\,cm^{-2}}$. The minimum surface density in the active layer, that occurs close to the inner edge of the dead zone, can be very small especially for high critical magnetic Reynolds number. This is not well represented by the assumed constant value.

3.2 Accretion Rate

The accretion rate through the active layer of the disc is approximately given by

$$\dot{M} = 3\pi\nu\Sigma_{\rm m}. \qquad (25)$$

In Fig. 5 we show the accretion rate as a function of radius in the disc for our fiducial model for varying critical magnetic Reynolds number in the high metallicity limit. The thin active layer severely limits the accretion rate over the dead zone by up to several orders of magnitude compared with that through the outer turbulent parts of the disc. These discs cannot be in steady state.

The mass in the dead zone must increase in time because it is continually supplied by the active layer. With sufficient accretion on to the disc, the outer parts of the dead zone can become gravitationally unstable. The extra heating from the viscosity due to self gravity can trigger the MRI and with the sudden increase in the turbulence a significant fraction of the disc is accreted in an outburst. After the outburst the disc cools, the dead zone reforms and the cycle repeats (Armitage, Livio & Pringle 2001; Zhu et al. 2009b). This outburst mechanism, known as the gravo-magneto instability, should be similar no matter how the extent of the dead zone is determined. The outbursts can be explained by plotting the accretion rate through the disc against the surface density at a fixed radius. There are two possible

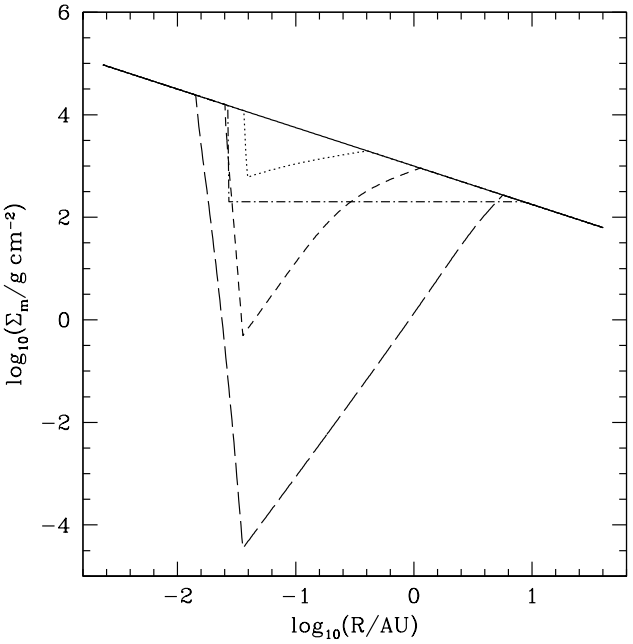

Figure 4. The total surface density (solid line) and the surface density in the active layer as a function of radius in the disc for critical magnetic Reynolds number of 1 (dotted line), 100 (short-dashed line) and 10^4 (long-dashed line) in the high metallicity limit. The inner parts of the disc are thermally ionised so $\Sigma_{\rm m} = \Sigma$ and similarly the outer parts of the disc are fully ionised by cosmic rays. The dot-dashed line shows the surface density in the active layer for the constant layer assumption where the disc is dead if $T < T_{\rm crit} = 1500\,{\rm K}$ and $\Sigma > \Sigma_{\rm crit} = 200\,{\rm g\,cm^{-2}}$.

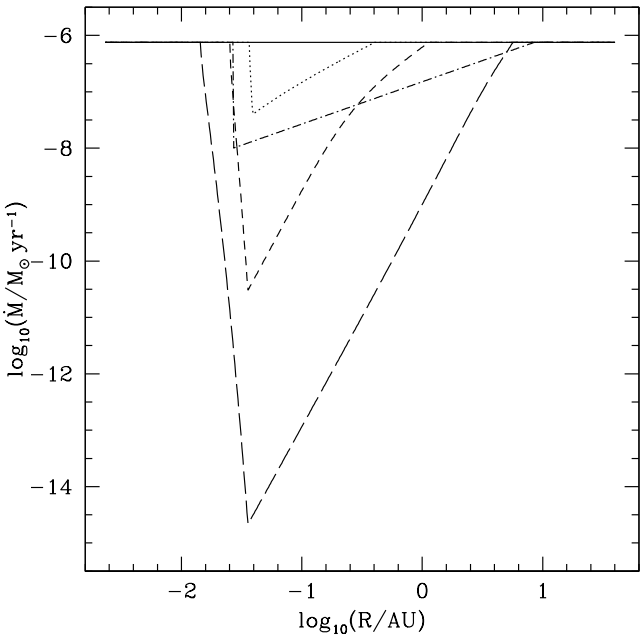

Figure 5. The accretion rate through the active layer of the disc in the high metallicity limit. The solid line shows a disc that is fully turbulent without a dead zone. The other three lines have a dead zone with a critical magnetic Reynolds number of 1 (dotted line), 100 (short-dashed line) and 10^4 (long-dashed line). These discs cannot be in steady state. The dot-dashed line shows the accretion rate through a disc with the constant surface density in the active layer (as in Fig. 4).

steady disc solutions, one that is fully turbulent and a second that is self gravitating. Outbursts occur when there is no steady solution for a given accretion rate at a specific radius. The disc moves between the two solutions in a limit cycle (Martin & Lubow 2011c).

The typical bolometric luminosity of protostars is smaller than would be expected from the infall rate and duration of the protostellar phase (Kenyon et al. 1990). Observations of T Tauri stars suggest that at an age of around 1 Myr the accretion rate through the disc is around $10^{-8}\,{\rm M_\odot\,yr^{-1}}$ (e.g. Valenti et al. 1993; Hartmann et al. 1998). One solution to this luminosity problem is thought to be time-dependent accretion on to the star that may be caused by dead zone formation in the disc. The disc spends the majority of its time with a dead zone and a restricted accretion rate on to the star. A low critical magnetic Reynolds number of around one could help to explain the observed accretion rates (see Fig. 5). In a time dependent disc, the accretion on to the central star will be of the order of the minimum accretion rate through the disc after a viscous timescale,

$$t_\nu = \frac{R^2}{\nu}, \tag{26}$$

at that radius. For example, at a radius of 0.1 AU, the viscous timescale is short at around 450 yr. It is difficult to reconcile a model with a high critical magnetic Reynolds number to the observations of T Tauri star accretion rates unless there is a source of external heating on the disc.

4 ANALYTIC APPROXIMATIONS

Fig. 4 suggests that the surface density in the active layer above the dead zone can be approximated by a power law in radius for high critical magnetic Reynolds numbers. When the surface density is sufficiently large, the active layer surface density is insensitive to the total surface density (as shown in Fig. 1). This, however, does not translate into the active layer surface density being constant in radius. As described in Section 3.1, the dominant effect is the scale height of the disc, H, that increases with radius leading to an increase in the active layer surface density.

An analytic approximation to the active layer surface density is found by neglecting the third term in equation (22) and then approximating $\Sigma_{\rm m} \propto \exp[-(z_{\rm crit}/H)^2/2]$. For cosmic ray ionisation

$$\Sigma_{\rm a,cr} = 1.36 \left(\frac{\alpha}{0.1}\right) \left(\frac{T}{100}\right)^2 \left(\frac{Re_{\rm M,crit}}{10^4}\right)^{-2} \left(\frac{M}{\rm M_\odot}\right)^{-\frac{3}{2}} \times \left(\frac{\zeta_0}{10^{-17}\,{\rm s^{-1}}}\right) \left(\frac{R}{1\,{\rm AU}}\right)^{9/2} {\rm g\,cm^{-2}}. \tag{27}$$

In regions where thermal ionisation is the dominant source,

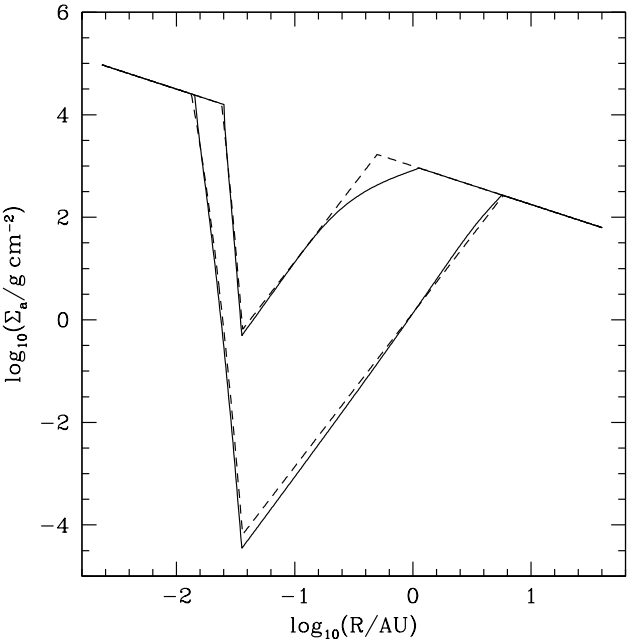

Figure 6. The surface density in the active layer. The solid lines show numerical solutions. The dashed lines show analytic approximations. The upper lines have $Re_{\rm M,crit} = 100$ and the lower lines have $Re_{\rm M,crit} = 10^4$.

the layer can be approximated with

$$\Sigma_{\rm a,t} = 0.2 \left(\frac{\alpha}{0.1}\right) \left(\frac{T}{1500}\right)^3 \left(\frac{Re_{\rm M,crit}}{10^4}\right)^{-2} \left(\frac{R}{0.03\,{\rm AU}}\right)^{9/2} \times \left(\frac{M}{{\rm M}_\odot}\right)^{-\frac{3}{2}} \exp\left[-25188\left(\frac{1}{T} - \frac{1}{1500}\right)\right] {\rm g\,cm^{-2}}. \quad (28)$$

Now we can fit the whole active layer surface density analytically. In Fig. 6 we show the analytic approximation to the surface density in the active layer is a good fit for high critical magnetic Reynolds number, $Re_{\rm M,crit} \gtrsim 100$. Note that even though we have only shown one temperature and surface density distribution in this work, these fits are valid for any distribution.

The accretion rate through the layer can be approximated by

$$\dot{M} = 1.0 \times 10^{-9} \left(\frac{\alpha}{0.1}\right)^2 \left(\frac{T}{100}\right)^3 \left(\frac{Re_{\rm M,crit}}{10^4}\right)^{-2} \times \left(\frac{M}{{\rm M}_\odot}\right)^{-2} \left(\frac{\zeta_0}{10^{-17}\,{\rm s^{-1}}}\right) \left(\frac{R}{1\,{\rm AU}}\right)^6 {\rm M_\odot\,yr^{-1}} \quad (29)$$

in regions where cosmic ray ionisation is the dominant source. The minimum accretion rate through the disc occurs where cosmic ray ionisation takes over from thermal ionisation. By finding where the surface densities in equations (27) and (28) are equal, we find this occurs at a temperature of $T \approx 10^3$ K. The radius corresponding to this temperature has the smallest accretion rate (see Fig. 5). As explained in Section 3.2, the accretion on to the central object will be limited by this minimum over a viscous timescale at that radius.

If the viscosity α parameter is smaller than the value we have taken in this work, of 0.1, then both the active layer surface density and accretion rate would be smaller than predicted here (see equations 27 and 28). The disc would become even more unstable to the gravo-magneto instability. The results shown here represent an upper limit to the surface density in the active layer.

5 DISCUSSION

There are three non-ideal MHD effects in the generalised Ohm's law, Ohmic resistivity, Hall effect and ambipolar diffusion, that dominate for different regimes. The Ohmic term, that we have used here, dominates at high density and very low ionisation. However, the ambipolar diffusion dominates for low density and high ionisation and the Hall effect dominates in a region between these two extremes (Wardle 1997). Recent work suggests that the MRI in the surface layers of discs may be dictated by ambipolar diffusion (Perez-Becker & Chiang 2011a,b; Bai & Stone 2011) or the Hall effect (Wardle & Salmeron 2011) rather than Ohmic resistivity as we have assumed here. Wardle & Salmeron (2011) applied a model with all three effects to the minimum mass solar nebula and found that at a radius of 1 AU there is around an order of magnitude increase or decrease in the active layer surface density, depending on whether the field is parallel or antiparallel to the rotation axis, respectively, compared with a disc with only Ohmic resistivity. These extra effects could change the surface density in the active layer and the accretion rate through the disc predicted here by around an order of magnitude. However, Ohmic resistivity has the advantage of being independent of the magnetic field (Fleming 2000) and the values it produces for the surface density of the active layer represent an average for the values obtained over a range of vertical magnetic fields (e.g. Wardle & Salmeron 2011).

Fromang, Terquem & Balbus (2002) use a similar approach to the work presented here but find that the active layer in the disc decreases with radius such that the dead zone surface density is approximately constant. The temperature distribution they use, shown in their Figure 1, has a very steep radial dependence in the region where the dead zone forms. With the analytical fits given here, it is clear that the constant active layer surface density can be recovered if the temperature of the disc has a radius dependence $T \propto R^{-9/4}$. If the power is even smaller, $< -9/4$, then the active layer will decrease with radius as found by Fromang, Terquem & Balbus (2002). The analytical fits presented here in Section 4 would provide an approximation to the disc in this case too because they can describe any surface density and temperature distribution.

If cosmic rays are present, the depth of the active layer is insensitive to the presence of X-rays because they do not penetrate so far. However, X-rays could still increase the ionisation fraction, and hence the associated effective α, in the active layer. Igea & Glassgold (1999) showed that the X-ray ionisation rate near the surface is significantly larger than that of cosmic rays. The accretion rate through the layer may be higher than predicted in equation (29) if this is taken into account and perhaps could help to explain the T Tauri accretion rates for higher critical magnetic Reynolds number.

Observed FU Orionis systems may be one manifestation of the time-dependent accretion phenomenon. These luminous young stellar objects are found in star forming regions (Hartmann & Kenyon 1996). Their optical brightness increases by five magnitudes or more on a timescale of years and decays on a timescale of 50-100 years (Herbig 1977). The timescale and brightness of accretion outbursts from the gravo-magneto instability are similar to the observed FU Orionis outbursts (Armitage, Livio & Pringle 2001; Zhu et al. 2009b). Time-dependent numerical simulations are needed to investigate these effects more fully in a disc with a dead zone determined by the critical magnetic Reynolds number. By comparing the resulting outbursts with FU Orionis observations the value of the critical magnetic Reynolds number may be further constrained.

6 CONCLUSIONS

A typical assumption used in time-dependent simulations of accretion discs with dead zones is that the surface density in the MRI active layer above the dead zone is constant with radius. However, when the dead zone is identified by the value of the critical magnetic Reynolds number including the effects of recombination, the active layer surface density is generally found to increase with radius. The constant layer is best reproduced with a low critical magnetic Reynolds number.

However, MHD simulations suggest the critical magnetic Reynolds number may be much higher. For higher critical magnetic Reynolds numbers, $Re_{\rm M,crit} \gtrsim 100$ we have found an analytical fit to the active surface density (equations 27 and 28) that will be a useful approximation in future time-dependent calculations. The dead zone structure is very sensitive to the value of the critical magnetic Reynolds number, as seen in Fig. 4, but the value is still uncertain and needs to be clarified in further work. However, this is complicated by the fact that the α parameter in the viscosity is also uncertain.

The metallicity variation between our galaxy, the LMC and the SMC is not significant enough to affect the expected size of the dead zone in a disc (ignoring possible differences in dust abundances). When comparing accretion discs in our galaxy with those in the LMC and SMC for example, the high metallicity limit will be appropriate. In order to explain the observed difference in disc lifetimes with metallicity (e.g. De Marchi, Panagia & Romaniello 2010, 2011) some other effect must be taken into account.

ACKNOWLEDGEMENTS

We acknowledge useful comments from the anonymous referee. RGM thanks the Space Telescope Science Institute for a Giacconi Fellowship. SHL acknowledges support from NASA grant NNX07AI72G. JEP thanks the Collaborative Visitor Program at STScI for its support and hospitality.

REFERENCES

Armitage P. J., Livio M., Pringle J. E., 2001, MNRAS, 324, 705
Bai X., Stone J. M., 2011, ApJ, 736, 144
Balbus S. A., Hawley J. F., 1991, ApJ, 376, 214
Balbus S. A., Hawley J. F., 2000, in Benz W., Kallenbach R., Lugamair G. W., eds, ISSI Space Sci. Ser. 9, From Dust to Terrestrial Planets, Kluwer, Dordrecht, p. 39
Balbus S. A., Terquem C., 2001, ApJ, 552, 235
Blaes O. M., Balbus S. A., 1994, ApJ, 421, 163
Brandenburg A., Nordland A., Stein R. F., Torkelsson U., 1995, ApJ, 446, 741
Davis S. W., Blaes O. M., Hirose S., Krolik J. H., 2009, ApJ, 703, 569
De Marchi G., Pangia N., Romaniello M., 2010, ApJ, 715, 1
De Marchi G., Panagia N., Romaniello M., Sabbi E., Sirianni M., Prada M., Pier G., Degl'Innocenti S., 2011, ApJ, 740, 11
Fleming T. P., Stone J. M., Hawley J. F., 2000, ApJ, 530, 464
Fromang S., Terquem C., Balbus S. A., 2002, MNRAS, 329, 18
Fromang S., Papaloizou J., Lesur G., Heinemann T., 2007, A&A, 476, 1123
Gammie C. F., 1996, ApJ, 457, 355
Gammie C. F., Menou K., 1998, ApJ, 492, 75
Guan X., Gammie C. F., Simon J. B., Johnson B. M., 2009, ApJ, 694, 1010
Hartmann L., Kenyon S. J., 1996, ARA&A, 34, 207
Hartmann L., Calvet N., Gullbring E., D'Alessio P., 1998, ApJ, 495, 385
Hawley J. F., Gammie C. F., Balbus S. A., 1995, ApJ, 440, 742
Herbig G. H., 1977, ApJ, 217, 693
Hernández J., Calvet N., Hartmann L., Muzerolle J., Gutermuth R., Stauffer J., 2009, ApJ, 707, 705
Igea J., Glassgold A. E., 1999, ApJ, 518, 848
Kenyon S. J., Hartmann L. W., Strom K. M., Strom S. E., 1990, AJ, 99, 869
King A. R., Pringle J. E., Livio M., 2007, MNRAS, 376, 1740
Koyama K., Maeda M., Ozaki M., Kamata Y., Tawara Y., Skinner S., Yamauchi S., 1994, PASJ, 46, L125
Lynden-Bell D., Pringle J. E., 1974, MNRAS, 168, 60
Martin R. G., Lubow S. H., 2011a, MNRAS, 413, 1447
Martin R. G., Lubow S. H., 2011b, MNRAS, in preparation
Martin R. G., Lubow S. H., 2011c, ApJ, 740, L6
Matsumura S., Pudritz R. E., 2003, ApJ, 598, 645
Matsumura S., Pudritz R. E., Thommes E. W., 2009, ApJ, 691, 1764
Millar T. J., Farquhar P. R. A., Willacy K., 1997, A&AS, 121, 139
Okuzumi S., Hirose S., 2011, ApJ, accepted, arXiv:1108.4892
Oppenheimer M., Dalgarno A., 1974, ApJ, 192, 29
Perez-Becker D., Chiang E., 2011a, ApJ, 727, 2
Perez-Becker D., Chiang E., 2011b, ApJ, 735, 8
Pringle J. E., 1981, ARA&A, 19, 137
Sano T., Miyama S. M., Umebayashi T., Nakono T., 2000, ApJ, 543, 486
Shakura N. I., Sunyaev R. A., 1973, A&A, 24, 337
Shu F. H., Adams F. C., Lizano S., 1987, ARA&A, 25, 23
Spitzer L. J., Tomasko M. G., 1968, ApJ, 152, 971

Spitzer L., Physical Processes in the Interstellar Medium, John Wiley & Sons, New York
Stone J. M., Hawley J. F., Gammie C. F., Balbus S. A., 1996, ApJ, 463, 656
Terquem C. E. J. M. L. J., 2008, ApJ, 689, 532
Turner N. J., Sano T., 2008, ApJ, 679, 131
Umebayashi T., Nakano T., 1988, Prog. Theo. Phys. Suppl., 96, 151
Umebayashi T., Nakano T., 1981, PASJ, 33, 617
Valenti J. A., Basri G., Johns C. M., 1993, AJ, 106, 2024
Wardle M., 1997, ASPC, 121, 561
Wardle M., 1999, MNRAS, 307, 849
Wardle M., Salmeron S., 2011, arXiv:1103.3562
Zhu Z., Hartmann L., Gammie C., 2009a, ApJ, 694, 1045
Zhu Z., Hartmann L., Gammie C., McKinney J. C., 2009b, ApJ, 701, 634